Hindawi Publishing Corporation
Journal of Nanomaterials
Volume 2008, Article ID 739613, 7 pages
doi:10.1155/2008/739613

Research Article

Properties Enhancement of PS Nanocomposites through the POSS Surfactants

Huei-Kuan Fu,[1] Shiao-Wei Kuo,[2] Ding-Ru Yeh,[1] and Feng-Chih Chang[1]

[1] *Institute of Applied Chemistry, National Chiao-Tung University, Hsinchu 300, Taiwan*
[2] *Center for Nanoscience and Nanotechnology, Department of Materials Science and Optoelectronic Engineering, National Sun Yat-Sen University, Kaohsiung, 804, Taiwan*

Correspondence should be addressed to Shiao-Wei Kuo, kuosw@faculty.nsysu.edu.tw

Received 5 August 2007; Accepted 5 February 2008

Recommended by Junlan Wang

Polyhedral oligomeric silsesquioxane (POSS)-clay hybrids of polystyrene are prepared by two organically modified clays using POSS-NH_2 and C_{20}-POSS as intercalated agents. X-ray diffraction (XRD) studies show the formation of these POSS/clay/PS nanocomposites in all cases with the disappearance of the peaks corresponding to the basal spacing of MMT. Transmission electronic microscopy (TEM) was used to investigate the morphology of these nanocomposites and indicates that these nanocomposites are composed of a random dispersion of exfoliated clay platelets throughout the PS matrix. Incorporation of these exfoliated clay platelets into the PS matrix led to effectively increase in glass transition temperature (T_g), thermal decomposition temperature (T_d), and the maximum reduction in coefficient of thermal expansion (CTE) is ca. 40% for the C_{20}-POSS/clay nanocomposite.

1. INTRODUCTION

Organic-inorganic hybrid materials are recognized as a new class of advanced material because they can be synthesized or processed using versatile approaches and own tunable properties [1, 2]. Clays have been extensively used as reinforcement agents to prepare polymer-layered silicate nanocomposites with improved thermal and mechanical properties [3–9]. The incorporation of clay into polymer matrix imparts unique physical and chemical properties was first reported by the Toyota Research Lab for Nylon 6/organoclay nanocomposites [10]. These improvements are related to the dispersion of the layered silicate in the polymer matrix. Typically, the chemical structure of montmorillonite (MMT) consists of two fused silica tetrahedral sheets sandwiching an edge-shared octahedral sheet of either magnesium or aluminum hydroxide. Generally, the naturally occurring clays are hydrophilic characters and require a modification by intercalating with amino acid, alkylammonium, or phosphonium salts to become organically compatible [11, 12]. The resulting organophilic galleries of the organically modified montmorillonite (OMMT) will enhance the compatibility with polymer [13]. Several methods to make polymer clay nanocomposites have been demonstrated, including solution mixing, melt blending, and in situ polymerization [14–16]. The interaction of layered silicates with polymers leads to two classes of hybrid materials. In the first class, denoted as intercalated hybrids, one or more polymer chains are inserted between the host layers, generating ordered lamella with the distance of a few nanometers. In the second, described as delaminated hybrids, silicate layers of 1 nm thickness are exfoliated and dispersed in the polymer matrix.

Polyhedral oligomeric silsesquioxane (POSS) reagents, monomers, and polymers are emerging as new chemical feedstocks for the preparation of organic-inorganic nanocomposites [17–21]. Silsesquioxane is the term for all structures with the formula $(RSiO_{1.5})_n$, where R is hydrogen or any alkyl, alkylene, aryl, arylene, or organic functional derivative groups. POSS compounds with diameters of 1–3 nm can be possibly considered the smallest particles of silica, but unlike silica, silicones, or fillers, POSS molecules contain either functionalized or unfunctionalized substituents at each of the corner silicon atoms. These substituents can compatibilize POSS molecules with polymers or monomers. POSS macromonomer and POSS-containing polymers inspires to prepare the functionalized POSS cages, which can be used as the intercalating agents of layered silicates to prepare the nanocomposites combining the two types of

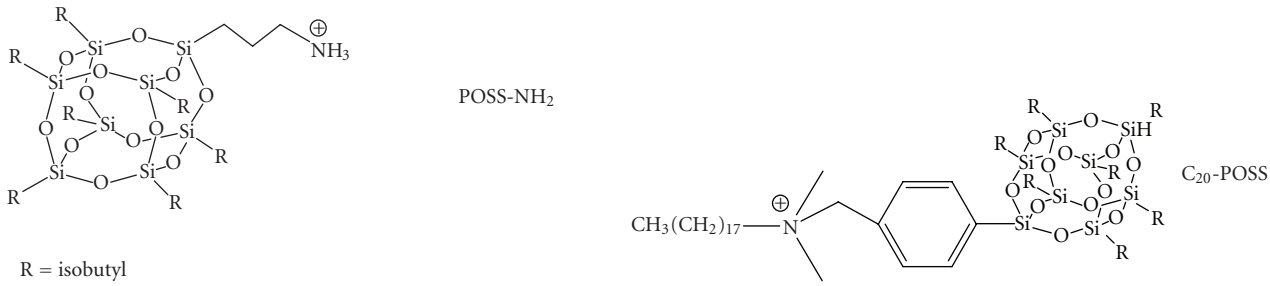

Scheme 1: Chemical structures of the intercalated agents used to prepare the modified clays.

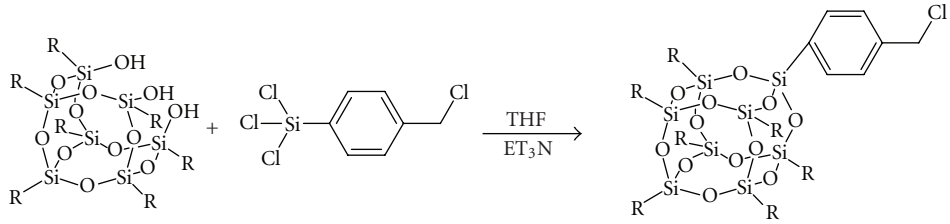

Scheme 2: Synthesis of POSS-Cl compound.

nanoreinforcement agents and improved mechanical and thermal properties.

In this study, these nanocomposites were prepared by emulsion polymerization using the POSS-NH_2 and C_{20}-POSS-treated clays as shown in Scheme 1. The morphology and the extent of delamination of the nanocomposites are elucidated using the X-ray diffraction and transmission electron microscopy. The thermal properties of these nanocomposites are characterized by thermalgravimetric analysis and differential scanning calorimetry. The coefficient of thermal expansion of virgin PS and nanocomposites are measured by thermal mechanical analyzer.

2. EXPERIMENTAL

2.1. Materials

The sodium montmorillonite (Na^+-MMT) with 1.45 mequiv/g cationic exchange capacity (CEC) was provided by Nanocor Co. (Ill, USA). The majority of chemicals used in this study including, acetone, methanol, tetrahydrofuran, acetonitrile, potassium hydroxide (KOH), triethylamine, and trichloro [4-(chloromethyl)phenyl] silane were acquired from Sigma-Aldrich Chemical Co., Inc. The styrene monomer was purchased from Sigma-Aldrich Chemical Co. and purified by removing the inhibitor with the aid of an inhibitor-removal column. Sodium dodecyl sulfate (SDS) and hydrochloride acid (HCl) were both obtained from Curtin Matheson Scientific, Inc. (Tex, USA). Potassium persulfate ($K_2S_2O_8$) and aluminum sulfate[$Al_2(SO_4)_3$] were acquired from Fisher Scientific, Inc. (Pittsburgh, USA). N, N-dimethyloctadecylamine (C_{20}) was obtained from Acros Organics, (NJ, USA). Trisilanolisobutyl polyhedral oligomeric silsesquioxane (T7-POSS) and aminopropylisobutyl polyhedral oligomeric silsesquioxane (POSS-NH_2) were obtained from Hybrid Plastic Corporate Headquarters Inc. (USA). All reagents, except styrene, were used as received without further purification.

2.2. Preparation of C_{20}-POSS intercalated agent

The POSS-Cl compound was prepared by the method based on Scheme 2 [22]. Trisilanolisobutyl polyhedral oligomeric silsesquioxane (3 g) and Et_3N (1.26 g) were added into a 100 mL two-neck round bottom flask and stirred continuously for 3 hours under nitrogen, then 20 mL of THF was added into the flask at 0°C for 1 hour. After stirring at 0°C under nitrogen, triethylamine, and trichloro[4-(chloromethyl) phenyl]silane(1.28 g) in THF (10 mL) were added dropwisely into the solution and stirred at 0°C. The cooling bath was removed and stirred continuously for 7.5 hours under nitrogen. The POSS-Cl compound and $HNEt_3$-Cl byproduct were separated by filtration. The clear THF solution was dropped into a beaker of acetonitrile and rapidly stirred. The resulting product was collected and dried in a vacuum oven for 24 hours. ^{1}H NMR (i.e., proton-NMR spectroscopy) ($CDCl_3$),δ: 7.59 (d, 2H), 7.33 (d, 2H), 4.52 (s, 2H), 1.92–1.62 (m, 7H), 1.09–0.85 (m, 42H), 0.75–0.48 (m, 14H).

The intercalated agent of C_{20}-POSS was prepared as shown in Scheme 2. N, N-dimethyloctadecylamine (C_{20}, 1.49 g) and POSS-Cl compound (5.68 g) in acetone (15 mL) were refluxed 80°C under nitrogen for 24 hours. After

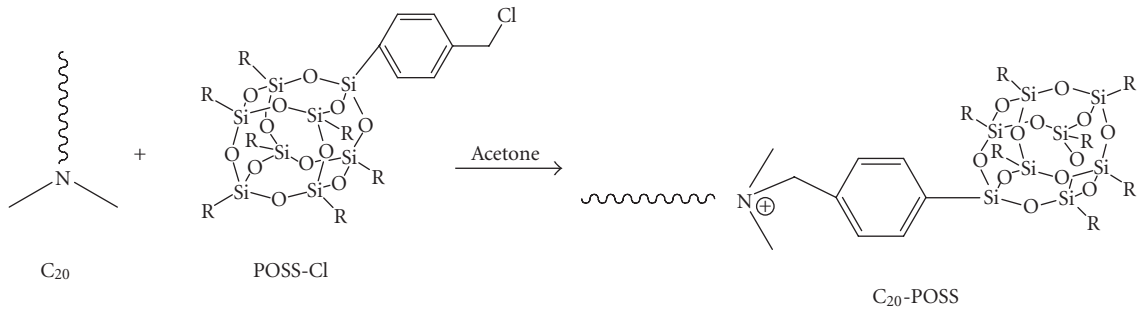

Scheme 3: Synthesis of the C_{20}-POSS intercalated agent.

cooling, the mixture was evaporated by a rotatory evaporator and then added Et_2O (20 mL). The solution was extracted with deionized water three times (150 mL×3). The organic phase was dried with $MgSO_4$ and evaporated by arotatory evaporator to obtain the C_{20}-POSS intercalated agent. ^{1}H NMR ($CDCl_3$), δ:7.68 (d, 2H), 7.58 (d, 2H), 5.03 (s, 2H), 3.42 (t, 2H), 3.30 (s, 6H), 1.81 (m, 7H), 1.41 (m, 2H), 1.26 (m, 30H), 0.90 (m, 42H), 0.82 (t, 3H), 0.59 (m, 14H).

2.3. Preparation of POSS-NH_2 and C_{20}-POSS Modified Clays

Na^+MMT (0.3 g) in deionized water (50 mL) was stirred continuously at 80°C for 4 hours. The POSS-NH_2 (0.38 g) or C_{20}-POSS (0.63 g) in water (5 mL) was placed into another flask and then 10% hydrochloric acid (1 mL) and ethanol (5 mL) were added and stirred at 80°C for 1 hour. This intercalated solution was poured slowly into the clay suspension solution and stirred vigorously at 80°C for 4 hours. The resulting white precipitate was separated by filtration and then washed thoroughly with warm deionized water. The final product was dried in a vacuum oven at room temperature overnight.

2.4. Preparation of Polystyrene/Clay Nanocomposites

Na^+-MMT (0.3 g) was dispersed in 40 mL of deionized water and stirred at 80°C for 4 hours. Based on the CEC value (145mequiv/100g) of the Na^+-MMT and the Mw of the intercalated agent, the calculated weight (the weight of the intercalated agent needed to fully replace the Na^+ of the clay) of the intercalated agent was added and stirred for 4 hours. KOH (0.02 g), SDS (0.4 g), $K_2S_2O_8$ (0.05 g), and styrene monomer (10 g) were added into the solution. After emulsification, the dispersion was flushed with nitrogen for 30 minutes while the temperature was raised to 80°C under nitrogen protection. Polymerization was carried out at 80°C for 8 hours. After cooling, 10 mL of the 2.5% aqueous aluminum sulfate was added into the polymerized emulsion, followed by dilute hydrochloric acid (10 mL) with stirring. Finally, acetone was added to break down the emulsion completely and then the polymer product was washed several times with methanol and deionized water. The white powder was filtered and dried in a vacuum oven at 80°C for 24 hours. Similar procedures were employed to prepare the virgin polystyrene.

2.5. Instrumentations

2.5.1. Measurement of the molecular weights characterization

Molecular weight (Mw), number-average(Mn) molecular weight, and polydispersity index (Mw/Mn) were measured using a Waters 410 gel permeation chromatography (GPC) system equipped with RI and UV detectors and a series of styragel columns (100, 500, and 10^3 Å). The system was calibrated using polystyrene standards. These polymer chains were extracted from the clay surface using a reverse ion exchange reaction with LiCl/DMF to determine the molecular weight and molecular weight distribution.

2.5.2. Structure analysis characterization

^{1}H NMR spectra were recoded in $CDCl_3$ on a Bruker AM 500 (500 MHz) spectrometer using the solvent signal as an internal standard. FT-IR spectra were recorded using a Nicolet Avatar 320 FT-IR spectrometer; 32 scans were collected at a spectral resolution of 1 cm^{-1}. The modified clay was mixed with KBr pellets to press into the small flakes and dried at 70°C for 24 hours. The holder was placed in the sample chamber and spectrum was recorded under N_2 purge to maintain the test of the sample dryness.

Transmission electron microscopy (TEM) images were obtained on a Hitachi H-7500 operating at 100 kV. The sample was thin section to ~70 nm by a Leica ultracut UCT microtome. Wide-angle X-ray diffraction (WAXD) experiments were carried on a Rigaku D/max-2500 type X-ray diffraction instrument with Cu Kα radiation (λ = 1.54 Å) using an Ni-filter. Data were recorded in the range of 2θ = 1 to 20 at the scanning rate of 0.6°/min.

2.5.3. Thermal and mechanical analysis characterization

Thermal stability of nanocomposite was investigated by a TA Instruments Q50 apparatus. The sample ~5 mg was placed in a Pt cell with scan rate of 20°C/min from 30 to 800°C under a 40 mL/min flow of nitrogen gas. Thermal analysis through differential scanning calorimetry (DSC) was performed using a Du-Pont (DSC-2010) to measure the glass transition temperature (T_g) of the nanocomposite. The sample was preheated at a scan rate of 20°C/min from 30 to 150°C under

a nitrogen atmosphere. A small sample (ca. 5–10 mg) was weighted and sealed in an aluminum pan. The sample was quickly cooled to 10°C from the first scan and then scanned between 30 and 150°C at the scan rate of 20°C/min. The glass transition temperatures are taken as the midpoint of the heat capacity transition between the upper and lower points of deviation from the extrapolated glass and liquid lines. The coefficient of thermal expansion (CTE) was measured using a thermomechanical analyzer (TMA TA 2940) by recording the change in dimension of the specimen with temperature. The specimen was heated from 25 to 150°C at a heating rate of 5°C/min.

3. RESULTS AND DISCUSSION

3.1. Morphologies of modified clays and nanocomposites

Microstructures of polymer-layered silicate nanocomposites were characterized by XRD and TEM. Figure 4 shows the X-ray diffraction curves of the pristine clay and modified clays in the 2θ region of 2–10°. For the pristine clay, the Bragg diffraction peak at $2\theta = 6.92°$ corresponds to d-spacing of 1.28 nm. For the POSS-NH_2/clay and C_{20}-POSS/clay, the 2θ value shifts from 6.92° (1.28 nm) to 5.51° (1.61 nm) and 2.33° (3.80 nm) after ion exchange, indicating that the basal spacing is expanded as the sodium cations in the interlayer galleries are replaced by intercalated agents of POSS-NH_2 and C_{20}-POSS. The increase of the basal spacing indicates that the clay can be efficiently intercalated by POSS-NH_2 and C_{20}-POSS. The d-spacing of the C_{20}-POSS-modified clay is substantially greater than the POSS-NH_2-modified clay. Larger interlayer spacing favors the penetration of styrene monomer and the formation of exfoliated nanocomposite by providing more hydrophobic environment. The pure POSS-NH_2 has characteristic diffraction peaks arising from the aggregation of the POSS [23]. Figure 5 shows XRD patterns of the unmodified clay and the C_{20}-POSS modified clay. The pure C_{20}-POSS has a broad peak in the region of 5–12° arising from the C_{20} long aliphatic chain. When the C_{20}-POSS is inserted between the galleries of the clay, the d spacing is increased from 1.28 nm for original clay to 3.80 nm, implying that the organic modifier is incorporated between and pushing the clay layers. Both nanocomposites do not show XRD diffraction peak as shown in Figure 6, indicating the silicate layers are exfoliated in the polymer matrix. TEM images for POSS-NH_2/clay and C_{20}-POSS/clay nanocomposites at 3% inorganic clay loading are shown in Figures 7(a) and 7(b), indicating that the exfoliated clay platelets are distributed in the matrix homogeneously and randomly.

3.2. Fourier transfer infrared analyses

The representative FT-IR spectra of the organophilic clay, POSS-NH_2-modified and C_{20}-POSS modified clays are given in Figure 1. After ion exchange, FT-IR spectroscopy can provide important information regarding the difference between intercalated agents and modified clays. In Figure 1(a), characteristic vibration bands of the pure clay are 1030 cm^{-1}(Si–O), 520 cm^{-1} (Al–O), and 470 cm^{-1} (Mg–O) [24–26]. In Figure 1(b), the absorption peaks in the region of 2950–2800 is assigned to the stretching vibration of aliphatic C–H. The symmetrical Si–O–Si band in the silsequioxane cage is characterized by the stretching band at 1109 cm^{-1}. In Figure 1(d), C_{20}-POSS contains both alkyl chain and POSS moiety where the POSS moiety exhibits characteristic absorption peaks at 2950–2800 cm^{-1} (C–H bonds), 1230 cm^{-1} (Si–C bonds), 1109 cm^{-1} (Si–O–Si bonds of the cage structure). The characteristics of the vibration band of alkyl chain appear at 2920, 2850, and 1475 cm^{-1} (–CH_2–vibration bands). Figures 1(c) and 1(e) show the features of combination of characteristic bands of pure clay, POSS-NH_2, and C_{20}-POSS. IR analysis further confirms the existence of these intercalated agents in

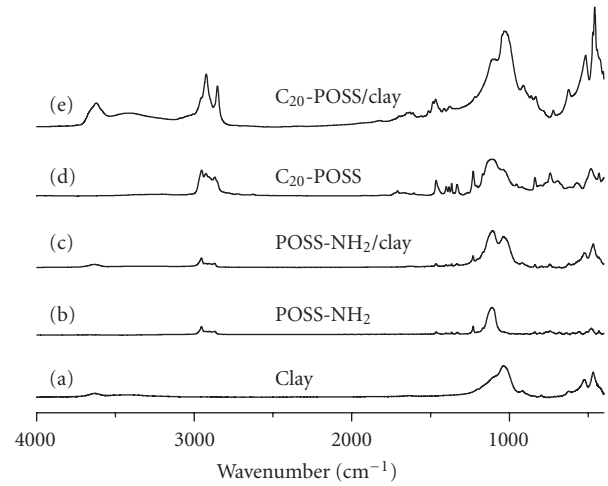

Figure 1: IR spectra of the two intercalated agent, intercalated clay, and pure clay.

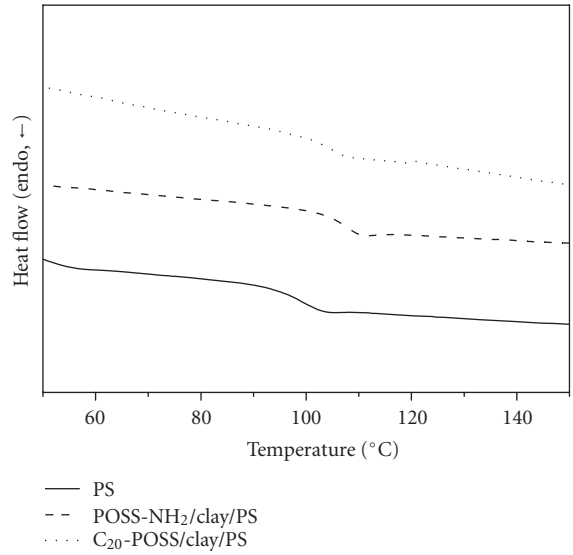

Figure 2: DSC curves glass transition temperature of (a) PS, (b) the nanocomposites formed used POSS-NH_2, and (c) the nanocomposites formed used C_{20}-POSS.

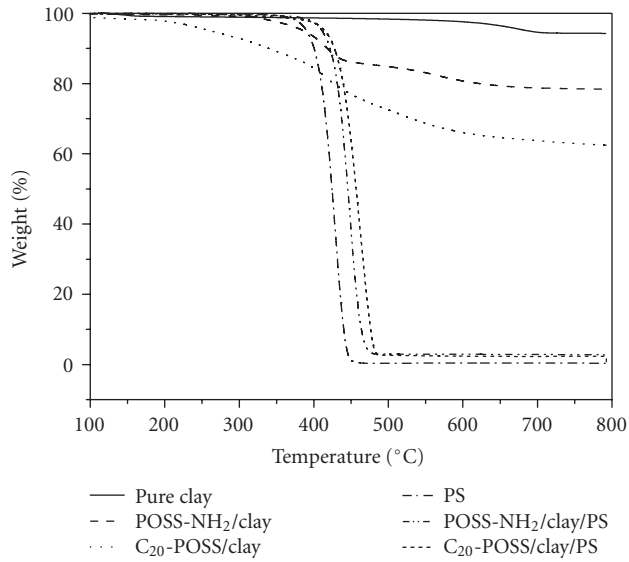

Figure 3: TGA curves of (a) pure Clay, (b) POSS-NH_2/Clay, (c) C_{20}-POSS/Clay, (d) pure PS, (e) the nanocomposite formed with POSS-NH_2, and (f) the nanocomposite formed with C_{20}-POSS.

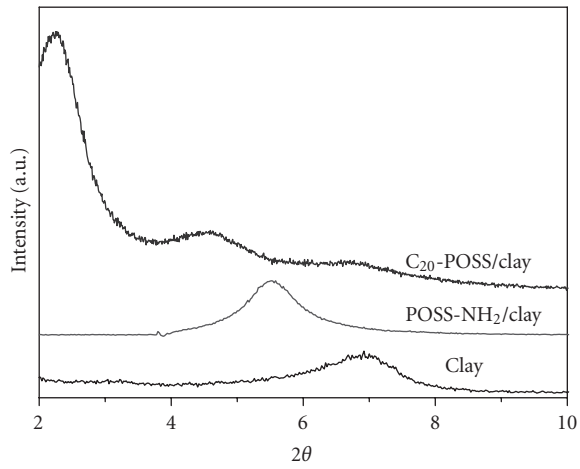

Figure 4: X-Ray diffraction patterns of pure clay, and intercalated clay.

these intercalated clay samples, implying that these intercalations of the intercalated agents are indeed present within the gallery gap. These observations support the explanation in the earlier observation from XRD.

3.3. Thermal properties

Figure 2 presents DSC traces of these nanocomposites with different intercalated agents. All DSC thermograms display single glass transition temperatures in the experimental temperature range. The glass transition temperature of PS occurs at 100°C. With the addition of the POSS and C_{20}-POSS modified MMT to the polymer matrix, the glass transition temperatures (T_gs) of the POSS-NH_2/clay/PS and C_{20}-

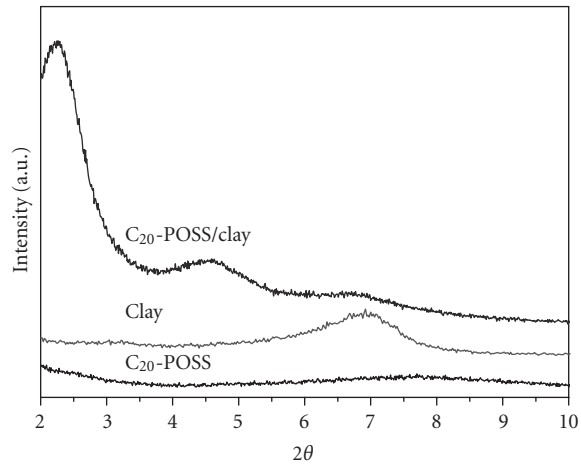

Figure 5: XRD spectra of C_{20}-POSS, pure clay, and C_{20}-POSS/Clay.

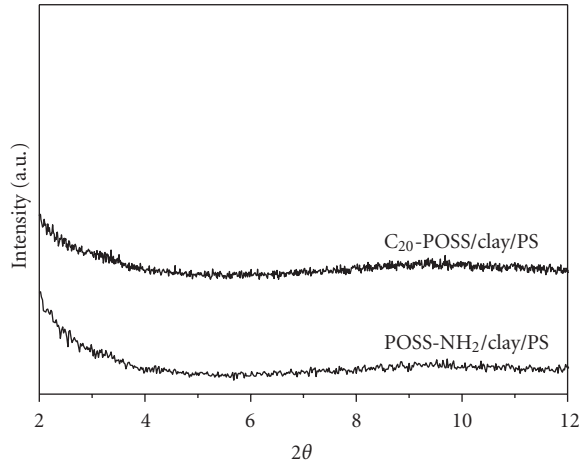

Figure 6: XRD spectra of the two surfactant-containing nanocomposites indicating the extent of delamination.

POSS/clay/PS are 108, and 105°C, respectively. From the DSC results that the incorporation of the organoclay resulted in an increase in the T_g relative to virgin PS, as summarized in Table 1. The addition of clay results in T_g increase which can be attributed to the retardation of PS chain movement.

Figure 3 presents the thermal stabilities of POSS-NH_2- and C_{20}-POSS-modified clays and nanocomposites investigated by TGA. Both nanocomposites show improved thermal stabilities than the virgin PS. The improvement in the degradation temperature is mainly due to the homogeneous dispersion of silicate nanoplatelets in the PS matrix [27–30]. In Figure 3, the C_{20}-POSS/clay decomposes at 262°C while the POSS-NH_2/clay decomposes at higher temperature of 38°C. The POSS-NH_2-modified clay is relatively more stable than the C_{20}-POSS-modified clay. Essentially, all nanocomposites give higher decomposition temperatures than the pristine PS and the improved thermal stability can be attributed to the diffusion hindrance of the decomposited volatiles. The values of 5% and 50% weight loss temperatures and the char yields are summarized in Table 1.

Table 1: Results of thermal and mechanical properties of polystyrene and polystyrene nanocomposites.

Sample	T_g,(°C)[a]	$T_{0.05}$,(°C)[b]	$T_{0.5}$,(°C)[c]	Char at 600(°C) %	CTE(μm/m°C)
PS	100 ± 0.5	390 ± 1.7	424 ± 0.8	0	164 ± 2
POSS/Clay/PS	108 ± 0.6	411 ± 1.3	446 ± 1.2	2.9	98 ± 1
C_{20}-POSS/Clay/PS	105 ± 0.3	415 ± 1.1	457 ± 0.9	2.4	100 ± 3

[a]Glass transition temperature (T_g).
[b]5% Degradation temperature ($T_{0.05}$).
[c]50% Degradation temperature ($T_{0.5}$).

Table 2: Molecular weights of polystyrene and polystyrene nanocomposites.

Sample	Mn ($\times 10^4$)[a]	Mw ($\times 10^4$)[b]	PDI (Mw/Mn)[c]
PS	34.5	53.1	1.54
POSS-NH_2/Clay/PS	40.9	54.0	1.32
C_{20}-POSS/Clay/PS	47.7	58.7	1.23

[a]Number-average molecular weights (Mn).
[b]Weight-average molecular weights (Mw) were determined by GPC.
[c]Polydispersity index, Mw/Mn.

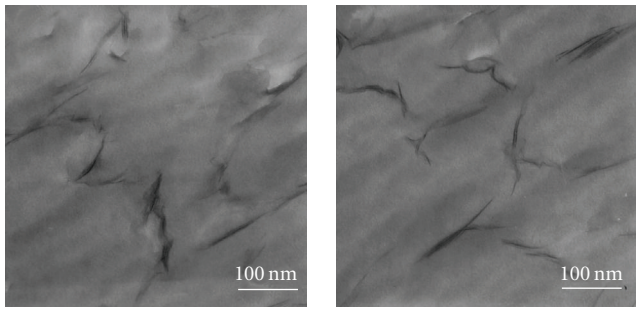

(a) (b)

Figure 7: TEM images of (a) POSS-NH_2 and (b) C_{20}-POSS-treated nanocomposites.

3.4. Molecular weights of the nanocomposites

Molecular weight and molecular weight distribution (PDI) by GPC analyses of polymer samples recovered after excluding all clay content are listed in Table 2. From Table 2, molecular weight (Mw or Mn) of the PS in the PS/clay nanocomposites is higher than the pure PS, suggesting that clay may act as a catalytic agent responsible for the observed higher molecular weight of the PS with the proceeding emulsion polymerization.

3.5. Coefficient of thermal coefficient

Thermal mechanical analyzer (TMA) was used to determine the coefficient of thermal expansion of the POSS/clay nanocomposites. The thermal expansion coefficient is an important issue for polymers in engineering applications. The CTE was measured from the initial linear slope of the thermal strain-temperature plot. A low thermal expansion coefficient is often desirable to achieve dimensional stability and can be achieved by incorporation of a rigid and low CTE filler material. From the data in Table 1, the CTE of the virgin PS is 164 μm/m°C and the addition 3 wt% organically modified clays reduces the CTE values to 98 and 100 μm/m°C for POSS/clay/PS and C_{20}-POSS/clay/PS approximately 40% reduction relative to the virgin PS.

In general, the extent of CTE reduction depends on the particle rigidity and fine dispersion of the clay platelets in the PS matrix and also due to efficient stress transfer to clay layers. The retardation of PS chain segmental movement through incorporation of organically modified clays also leads to decrease in the coefficient of thermal expansion (CTE). The incorporation of the organically modified clays results in significant improvement in dimensional stability of the PS matrix.

4. CONCLUSIONS

The POSS-clay hybrids of polystyrene are prepared via emulsion polymerization using two organically modified clays, POSS-NH_2 and C_{20}-POSS, as intercalated agents. X-ray diffraction (XRD) results indicate that the clay is successfully intercalated by POSS-NH_2 and C_{20}-POSS. The random dispersion of these exfoliated silicate layers in these nanocomposites are identified by XRD and TEM. These well dispersed clay platelets in PS matrix result in improved thermal properties in terms of thermal decomposition temperature (T_d) and glass transition temperature (T_g). In addition, the incorporation of these organoclay results in significant reduction in coefficient of thermal expansion of virgin PS.

ACKNOWLEDGMENT

This work was financially supported by the National Science Council, Taiwan , under Contracts no. NSC-96-2120-M-009-009 a nd NSC-96-2218-E-110-008.

REFERENCES

[1] H.-A. Klok and S. Lecommandoux, "Supramolecular materials via block copolymer self-assembly," *Advanced Materials*, vol. 13, no. 16, pp. 1217–1229, 2001.

[2] C. Sanchez, G. J. de A. A. Soler-Illia, F. Ribot, T. Lalot, C. R. Mayer, and V. Cabuil, "Designed hybrid organic-inorganic nanocomposites from functional nanobuilding blocks," *Chemistry of Materials*, vol. 13, no. 10, pp. 3061–3083, 2001.

[3] C. Park, J. G. Smith Jr., J. W. Connell, S. E. Lowther, D. C. Working, and E. J. Siochi, "Polyimide/silica hybrid-clay nanocomposites," *Polymer*, vol. 46, no. 23, pp. 9694–9701, 2005.

[4] D.-R. Yei, S.-W. Kuo, H.-K. Fu, and F.-C. Chang, "Enhanced thermal properties of PS nanocomposites formed from montmorillonite treated with a surfactant/cyclodextrin inclusion complex," *Polymer*, vol. 46, no. 3, pp. 741–750, 2005.

[5] W. Xie, J. M. Hwu, G. J. Jiang, T. M. Buthelezi, and W.-P. Pan, "A study of the effect of surfactants on the properties of polystyrene-montmorillonite nanocomposites," *Polymer Engineering & Science*, vol. 43, no. 1, pp. 214–222, 2003.

[6] D.-R. Yei, S.-W. Kuo, Y.-C. Su, and F.-C. Chang, "Enhanced thermal properties of PS nanocomposites formed from inorganic POSS-treated montmorillonite," *Polymer*, vol. 45, no. 8, pp. 2633–2640, 2004.

[7] C.-R. Tseng, J.-Y. Wu, H.-Y. Lee, and F.-C. Chang, "Preparation and characterization of polystyrene-clay nanocomposites by free-radical polymerization," *Journal of Applied Polymer Science*, vol. 85, no. 7, pp. 1370–1377, 2002.

[8] S. Su and C. A. Wilkie, "Exfoliated poly(methyl methacrylate) and polystyrene nanocomposites occur when the clay cation contains a vinyl monomer," *Journal of Polymer Science A*, vol. 41, no. 8, pp. 1124–1135, 2003.

[9] M. H. Kim, C. I. Park, W. M. Choi, et al., "Synthesis and material properties of syndiotactic polystyrene/organophilic clay nanocomposites," *Journal of Applied Polymer Science*, vol. 92, no. 4, pp. 2144–2150, 2004.

[10] A. Okado, M. Kawasumi, T. Kurauchi, and O. Kamigaito, "Synthesis and characterization of a nylon 6-clay hybrid," *Polymer Preprints*, vol. 28, pp. 447–448, 1987.

[11] D. Kong and C. E. Park, "Real time exfoliation behavior of clay layers in epoxy-clay nanocomposites," *Chemistry of Materials*, vol. 15, no. 2, pp. 419–424, 2003.

[12] W.-B. Xu, S.-P. Bao, and P.-S. He, "Intercalation and exfoliation behavior of epoxy resin/curing agent/montmorillonite nanocomposite," *Journal of Applied Polymer Science*, vol. 84, no. 4, pp. 842–849, 2002.

[13] A. Akelah, "Nanocomposites of grafted polymers onto layered silicates," in *Polymers and Other Advanced Materials: Emerging Technologies and Business Opportunities*, P. N. Prasad, J. E. Mark, and J. F. Tung, Eds., pp. 625–644, Plenum Press, New York, NY, USA, 1995.

[14] R. A. Vaia, S. Vasudevan, W. Krawiec, L. G. Scanlon, and E. P. Giannelis, "New polymer electrolyte nanocomposites: melt intercalation of poly(ethylene oxide) in mica-type silicates," *Advanced Materials*, vol. 7, no. 2, pp. 154–156, 1995.

[15] E. P. Giannelis, "Polymer layered silicate nanocomposites," *Advanced Materials*, vol. 8, no. 1, pp. 29–35, 1996.

[16] J. W. Gilman, A. B. Morgan, R. H. Harris, P. C. Trulove, H. C. Delong, and T. E Sutto, "Polymer layered silicate nanocomposites: thermal stability of organic cationic treatments," *Polymeric Materials Science and Engineering*, vol. 83, pp. 59–60, 2000.

[17] J. D. Lichtenhan, N. Q. Vu, J. A. Carter, J. W. Gilman, and F. J. Feher, "Silsesquioxane-siloxane copolymers from polyhedral silsesquioxanes," *Macromolecules*, vol. 26, no. 8, pp. 2141–2142, 1993.

[18] J. D. Lichtenhan, Y. A. Otonari, and M. J. Carr, "Linear hybrid polymer building blocks: methacrylate-functionalized polyhedral oligomeric silsesquioxane monomers and polymers," *Macromolecules*, vol. 28, no. 24, pp. 8435–8437, 1995.

[19] T. S. Haddad and J. D. Lichtenhan, "The incorporation of transition metals into polyhedral oligosilsesquioxane polymers," *Journal of Inorganic Organometallic Polymer*, vol. 5, no. 3, pp. 237–246, 1995.

[20] R. A. Mantz, P. F. Jones, K. P. Chaffee, et al., "Thermolysis of polyhedral oligomeric silsesquioxane (POSS) macromers and POSS-siloxane copolymers," *Chemistry of Materials*, vol. 8, no. 6, pp. 1250–1259, 1996.

[21] T. S. Haddad and J. D. Lichtenhan, "Hybrid organic-inorganic thermoplastics: styryl-based polyhedral oligomeric silsesquioxane polymers," *Macromolecules*, vol. 29, no. 22, pp. 7302–7304, 1996.

[22] C.-F. Huang, S.-W. Kuo, F.-J. Lin, et al., "Influence of PMMA-chain-end tethered polyhedral oligomeric silsesquioxanes on the miscibility and specific interaction with phenolic blends," *Macromolecules*, vol. 39, no. 1, pp. 300–308, 2006.

[23] H. Zhang, C. Wang, M. Li, X. Ji, J. Zhang, and B. Yang, "Fluorescent nanocrystal-polymer composites from aqueous banocrystals: methods without ligand exchange," *Chemistry of Materials*, vol. 17, no. 19, pp. 4783–4788, 2005.

[24] J.-M. Yeh, S.-J. Liou, C.-Y. Lai, P.-C. Wu, and T.-Y. Tsai, "Enhancement of corrosion protection effect in polyaniline via the formation of polyaniline-clay nanocomposite materials," *Chemistry of Materials*, vol. 13, no. 3, pp. 1131–1136, 2001.

[25] J.-M. Yeh, S.-J. Liou, C.-Y. Lin, C.-Y. Cheng, Y.-W. Chang, and K. R. Lee, "Anticorrosively enhanced PMMA-clay nanocomposite materials with quaternary alkylphosphonium salt as an intercalating agent," *Chemistry of Materials*, vol. 14, no. 1, pp. 154–161, 2002.

[26] J.-M. Yeh, C.-L. Chen, Y.-C. Chen, et al., "Enhancement of corrosion protection effect of poly(*o*-ethoxyaniline) via the formation of poly(*o*-ethoxyaniline)-clay nanocomposite materials," *Polymer*, vol. 43, no. 9, pp. 2729–2736, 2002.

[27] P. Uthirakumar, K. S. Nahm, Y. B. Hahn, and Y.-S. Lee, "Preparation of polystyrene/montmorillonite nanocomposites using a new radical initiator-montmorillonite hybrid via in situ intercalative polymerization," *European Polymer Journal*, vol. 40, no. 11, pp. 2437–2444, 2004.

[28] T. K. Chen, Y. I. Tien, and K. H. Wei, "Synthesis and characterization of novel segmented polyurethane/clay nanocomposite via poly(ε-caprolactone)/clay," *Journal of Polymer Science A*, vol. 37, no. 13, pp. 2225–2233, 1999.

[29] J. G. Doh and I. Cho, "Synthesis and properties of polystyrene-organoammonium montmorillonite hybrid," *Polymer Bulletin*, vol. 41, no. 5, pp. 511–518, 1998.

[30] X. Fu and S. Qutubiddin, "Polymer-clay nanocomposites: exfoliation of organophilic montmorillonite nanolayers in polystyrene," *Polymer*, vol. 42, no. 2, pp. 807–813, 2001.

Research Letters in Materials Science

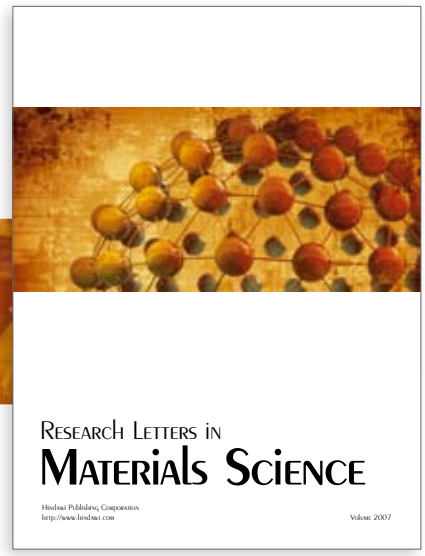

Why publish in this journal?

Research Letters in Materials Science is devoted to very fast publication of short, high-quality manuscripts in the broad field of materials science. Manuscripts should not exceed 4 pages in their final published form. Average time from submission to publication shall be around 60 days.

Why publish in this journal?

Wide Dissemination

All articles published in the journal are freely available online with no subscription or registration barriers. Every interested reader can download, print, read, and cite your article

Quick Publication

The journal employs an online "Manuscript Tracking System" which helps streamline and speed the peer review so all manuscripts receive fast and rigorous peer review. Accepted articles appear online as soon as they are accepted, and shortly after the final published version is released online following a thorough in-house production process.

Professional Publishing Services

The journal provides professional copyediting, typesetting, graphics, editing, and reference validation to all accepted manuscripts.

Keeping Your Copyright

Authors retain the copyright of their manuscript, which are published using the "Creative Commons Attribution License," which permits unrestricted use of all published material provided that it is properly cited.

Extensive Indexing

Articles published in this journal will be indexed in several major indexing databases to ensure the maximum possible visibility of each published article.

Submit your Manuscript Now...

In order to submit your manuscript, please visit the journal's website that can be found at **http://www.hindawi.com/journals/rlms/** and click on the "Manuscript Submission" link in the navigational bar.

Should you need help or have any questions, please drop an email to the journal's editorial office at **rlms@hindawi.com**

ISSN: 1687-6822; e-ISSN: 1687-6830; doi:10.1155/RLMS

Hindawi Publishing Corporation
410 Park Avenue, 15th Floor, #287 pmb, New York, NY 10022, USA
HINDAWI